

# Magnetic phases of magnetic polarons in diluted magnetic semiconductor nanocrystals

Shun-Jen Cheng\*

Department of Electrophysics, National Chiao Tung University, Hsinchu 30050, Taiwan

Received 25 April 2008, revised 2 October 2008, accepted 28 October 2008

Published online 16 December 2008

PACS 75.30.Hx, 75.50.Pp, 75.75.+a

\* e-mail sjcheng@mail.nctu.edu.tw, Phone: +886-3-5712121x56168, Fax: +886-3-5725230

We present theoretical studies of magnetism in II-VI magnetic nanocrystals (NCs) containing single electron coupled to substitutional magnetic ions  $\text{Mn}^{2+}$ . By using exact diagonalization techniques, we explore the magnetic phases of magnetic polarons in NCs doped with few  $\text{Mn}^{2+}$  ions, as functions of NC size, Mn number and positions. We show that ferromagnetic magnetic polarons (MPs) are stably formed in small magnetic NCs due to strong quantum confinement.

By contrast, magnetic polarons with short ranged Mn-clusters in larger NCs exhibit various distinct magnetic phases, from ferromagnetism (FM) to anti-ferromagnetism (AF), sensitively depending on NC size. The stability of magnetic polarons in NCs with arbitrary number of Mn ions are analyzed within a proposed solvable model, supported by the numerical results calculated by using local mean field theory (MFT).

© 2009 WILEY-VCH Verlag GmbH & Co. KGaA, Weinheim

**1 Introduction** Spin interactions are known to play an essential role in the carrier-mediated magnetism of diluted magnetic semiconductors (DMSs) [1]. In III-V DMSs, magnetic ion dopants, typically  $\text{Mn}^{2+}$  with spin  $5/2$ , act as acceptors providing not only the  $sp-d$  spin interaction with itinerant carriers but also additional attractive potentials to them [2]. The spin interactions between carriers and localized magnetic dopant in III-V DMSs can be further enhanced as holes are bound by  $\text{Mn}^{2+}$  acceptors due to the high local density at Mn site, i.e. forming magnetic polarons (MPs). Fascinating magnetic properties such as high  $T_c$  ferromagnetism of III-V DMSs, especially in the insulating regime or in that of near metal-insulating transition, are related to the formation of bound magnetic polarons [3]. As compared with III-V DMSs, such bound magnetic polarons however are not necessarily formed stably in II-VI DMSs because divalent Mn ions are isoelectronic in II-VI materials. Recent experimental and theoretical studies nevertheless suggest that the magnetic properties of II-VI DMSs could be optimized by reducing the dimensionality of DMS material, e.g. quantum dot,

with the stable formation of magnetic polarons improved by quantum confinement [4–6].

In this work, we present theoretical studies of carrier-mediated magnetism in II-VI magnetic nanocrystal quantum dots containing single electron coupled to arbitrary number of magnetic ions  $\text{Mn}^{2+}$ . By using exact diagonalization techniques, we calculate the energy spectra and magnetization of NCs doped with few Mn's (up to Mn number  $N_{\text{Mn}} = 3$ ). We show that ferromagnetic magnetic polarons (MPs) are stably formed in small magnetic NCs with isoelectronic Mn's due to strong quantum confinement of NCs. Remarkably, magnetic polarons with short ranged Mn-clusters in larger NCs exhibit various distinct magnetic phases, from ferromagnetism (FM) to anti-ferromagnetism (AF), controllable by engineering NC size and Mn positions. The stability of magnetic polarons in NCs with arbitrary number of Mn ions are analyzed within a proposed solvable model, supported by the numerical results calculated by using local mean field theory (MFT).

**2 Model Hamiltonian** We start with the Hamiltonian for a magnetic NC containing a single electron coupled to many magnetic ions, given by

$$H = |\mathbf{p}|^2/(2m^*) + V_0(\mathbf{r}) - \sum_I |J_{eM}^{(0)}| \mathbf{s} \cdot \mathbf{M}_I \delta(\mathbf{r} - \mathbf{R}_I) + \frac{1}{2} \sum_{I \neq J} |J_{MM}(R_{IJ})| \mathbf{M}_I \cdot \mathbf{M}_J, \quad (1)$$

where  $m^*$  is the effective mass of electron,  $V_0(\mathbf{r})$  the effective confining potential of NC,  $\mathbf{s}(\mathbf{M}_I)$  denotes the spin of electron (the spin of the  $I$ -th Mn ion at position  $\mathbf{M}_I$ ),  $\mathbf{r}$  ( $\mathbf{p}$ ) the position (momentum) coordinate of electron. The third (fourth) term describes contact ferromagnetic interaction between electron and  $\text{Mn}^{2+}$  (short ranged anti-ferromagnetic interaction between Mn's). The Mn-Mn interactions are mainly mediated by the superexchange mechanism, an indirect Coulomb exchange interaction mediated by anions [1,7]. Experimental measurements show that the typical values of the nearest neighbor Mn-Mn interactions in most II-VI:Mn alloys are at the scale of  $10^{-1} - 10^0$  meV, decaying rapidly with increasing Mn-Mn distance [1,7]. Throughout this work, we take  $J_{eM}^{(0)} = 10.8 \text{ meV} \cdot \text{nm}^3$  and  $J_{MM}(R_{IJ}) = J_{MM}^{(0)} \exp[-\lambda(R_{IJ}/a_0 - 1)]$  with the nearest neighbor Mn-Mn exchange energy  $J_{MM}^{(0)} = 0.5 \text{ meV}$  and  $\lambda = 5.1$ , where  $R_{IJ} \equiv |\mathbf{R}_I - \mathbf{R}_J|$  denotes the distance between two Mn ions and  $a_0 = 0.55 \text{ nm}$  lattice constant of NC material [8].

Taking the hard wall spherical model for effective confining potential  $V_0$  [9–11], we have the single electron wave functions and eigen energies of spherical NCs, explicitly given by  $E_{nlm} = \frac{\hbar^2 \alpha_{nl}^2}{2m^* a^2}$  and  $\psi_{nlm}(\mathbf{r}) = \langle \mathbf{r} | nlm \rangle = \sqrt{\frac{2}{a^3}} \frac{J_l(\frac{\alpha_{nl} r}{a})}{J_{l+1}(\alpha_{nl})} Y_{lm}(\theta, \psi)$ , respectively, where  $\mathbf{r} = (r, \theta, \phi)$  is the position of electron in polar coordinate,  $a$  the radius of spherical NC,  $J_l(r)$  the spherical Bessel function,  $\alpha_{nl}$  the  $n$ th zero of  $J_l$ , and  $Y_{lm}(\theta, \psi)$  the spherical Harmonic function,  $n$  is the principal quantum number,  $l$  the angular momentum,  $m$  the  $z$ -component of angular momentum.

### 3 Numerical results and analysis

**3.1 Exact diagonalization** To find the energy spectra of NCs with few Mn ions at high accuracy, we use the exact diagonalization technique for solving the eigenvalue problem for Eq. (1). We take the outer product of few single electron orbitals and *all* possible Mn spin configurations as basis, i.e.  $|nlm; s_z\rangle \otimes |M_1^z, M_2^z, \dots, M_N^z\rangle$ , build up the Hamiltonian matrix for Eq. (1), and finally carry out direct diagonalization. Convergence of numerical results is tested by increasing number of electron orbitals taken for the construction of e-Mn configurations. Since the typical energy quantization (at the scale of  $\sim 10^2$  meV) of NCs has two order of magnitude larger than e-Mn and Mn-Mn interactions ( $\sim 10^0$  meV), a single electron in magnetic NCs is nearly frozen in the lowest orbital and the satisfactory nu-

merical convergence is achieved even only one electronic orbital (i.e. the lowest s-orbital  $|100\rangle$ ) is taken.

Figure 1(a) shows the calculated low-lying energy spectra (relative to the ground state energy) of singly charged NCs doped with three long ranged  $\text{Mn}^{2+}$  ions at  $\mathbf{R}_1 = (X_1, Y_1, Z_1) = (a/2, 0, 0)$ ,  $\mathbf{R}_2 = (-a/2, 0, 0)$  and  $\mathbf{R}_3 = (0, 0, a/2)$ , respectively. With the long spatial separation between Mn's ( $a \gg a_0$  and  $J_{MM} \rightarrow 0$ ), the FM e-Mn interactions are predominant and give rise to magnetic ordering of Mn spins, i.e. forming ferromagnetic MPs with total spin  $M_{GS} = 5N_{Mn}/2 = 15/2$ . Figure 2 shows the calculated binding energies of the 3-Mn MPs, defined by  $E_b \equiv E_{GS}(J_{eM} \rightarrow 0) - E_{GS}$ , as function of NC radius, where  $E_{GS}$  is the ground state (GS) energy of system and  $E_{GS}(J_{eM} \rightarrow 0)$  is the energy of the lowest states calculated with disabling the e-Mn coupling. The binding energies  $E_b$  are positive over the range of NC sizes under consideration and increase with decreasing NC size. Significant increase of  $E_b$  is observed as NC size is smaller than the effective Bohr radius  $a < a_B \sim 3.1 \text{ nm}$  (here  $m^* = 0.15m_0$  and the dielectric constant  $\epsilon = 8.9$  are taken for CdSe NCs).

In reality, Mn ions are likely randomly distributed in NCs. To explore the effects of disorder, we study another case of non-uniformly Mn-doped NC. Figure 1(b) shows the numerically calculated relative energy spectra of singly charged NCs containing three nearest neighbor (NN) Mn's at  $\mathbf{R}_1 \sim \mathbf{R}_2 \sim \mathbf{R}_3 \sim (a/2, 0, 0)$ . The NCs with short ranged Mn-clusters are found to exhibit distinctive magnetic phases, from anti-ferromagnetism ( $M = 0$ ) to ferromagnetism ( $M = 15/2$ ), sensitively depending on NC size. This is because, with decreasing NC size, FM e-Mn interaction increases its strength and eventually become comparable to or even overwhelm the strong AF interactions between the nearest neighbor Mn's.

**3.2 A solvable simplified model** We see from Fig. 2 that the quantum size effect of small NCs drives MPs into FM phases and results in rapid increase of  $E_b$  (at the scale above  $> 10^1$  meV) regardless of Mn disorder. To gain more physical insights, we carry out an analysis based on a solvable model Hamiltonian [12]

$$H_{eff} = -|J_c| \mathbf{s} \cdot \mathbf{M} + \frac{|J_M|}{2} \sum_{I \neq J} \mathbf{M}_I \cdot \mathbf{M}_J, \quad (2)$$

in which constant e-Mn and Mn-Mn interactions are assumed. Here we can take the estimates for the coupling constants  $J_c \approx J_{eM}^{(0)}/\Omega_{NC}$  and  $J_M \approx J_{MM}(\langle R_{IJ} \rangle) \propto \exp[-\lambda(4x_{Mn})^{-1/3}]$ , where  $\Omega_{NC} = 4\pi a^3/3$  is the volume of NC,  $\langle R_{IJ} \rangle$  indicates the averaged value of Mn-Mn distance, and  $x_{Mn}$  is the fractional composition of Mn. It is clear that  $J_c$  ( $J_M$ ) increases with decreasing NC size (with increasing Mn concentration and/or decreasing NC size). Following Ref.[12], we have the eigen energies of the low lying states:  $E(J = M + \frac{1}{2}, M) =$

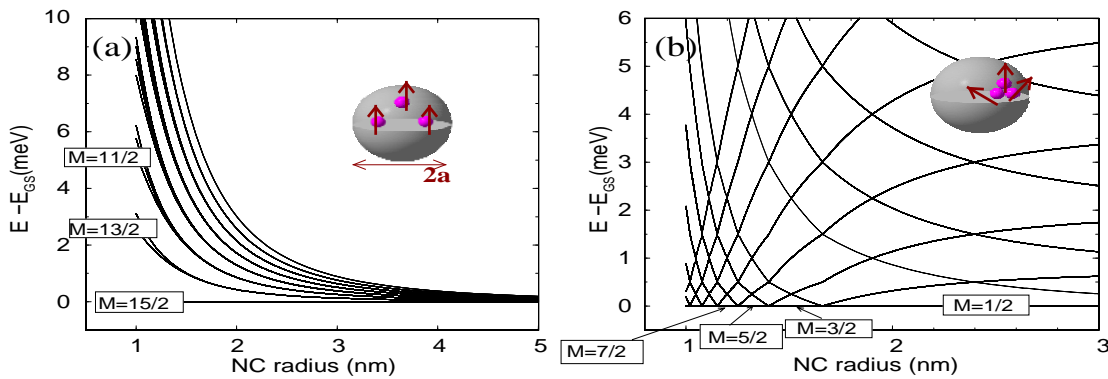


**Figure 1** The energy spectra relative to the ground state (GS) energies of singly charged NCs with various sizes doped with (a) three Mn ions positioned at  $\mathbf{R}_1 = (X_1, Y_1, Z_1) = (a/2, 0, 0)$ ,  $\mathbf{R}_2 = (-a/2, 0, 0)$  and  $\mathbf{R}_3 = (0, 0, a/2)$ , and (b) three nearest neighbor Mn ions at  $\mathbf{R}_1 \sim \mathbf{R}_2 = (a/2, 0, 0) \sim \mathbf{R}_3 = (a/2, 0, 0)$ . The results are calculated by using exact diagonalization. The GSs of the NCs containing the long ranged Mn's are stably in the FM phases. By contrast, the ground states of the NCs with three short ranged Mn's undergo a series of magnetic phase transitions, from anti-ferromagnetism (AF) to ferromagnetism (FM) with decreasing NC size.

$-\frac{J_c}{2}M + \frac{J_M}{2}[M(M+1) - 35N_{Mn}/4]$ . The total Mn spin of GS,  $M_{GS}$ , is determined by solving  $\frac{\partial E}{\partial M}|_{M=M_0} = 0$  and chosen as the integer (half-integer) value closest to  $M_0$  for even (odd) number of Mn. Accordingly, one can derive that  $M_{GS} = \text{integer part}[J_c/J_M + c] - c$ , where  $c = 0(1/2)$  for even (odd) number of Mn. The binding energy of magnetic polaron, defined by  $E_b \equiv E_{GS}(J_c \rightarrow 0) - E_{GS}$ , is given by

$$E_b = \frac{J_c}{2}M_{GS} - \frac{J_M}{2}[M_{GS}(M_{GS} + 1) - c'], \quad (3)$$

where  $c' = 0(3/4)$  for even (odd) number of Mn. Accordingly, we have the binding energies of three Mn MPs in FM phase estimated by

$$E_b = \frac{15J_c}{4} - \frac{63J_M}{2} \sim \left(\frac{45}{16\pi}\right) \cdot \frac{J_{eM}^{(0)}}{a^3} - \frac{63J_{MM}(\langle R_{IJ} \rangle)}{2}, \quad (4)$$

where the first (second) term is the positive (negative) contribution from the FM e-Mn (AF Mn-Mn) interaction to MP binding energy, tunable by NC size (averaged Mn concentration and spatial distribution). With the parameters for CdSe:Mn NCs used in this work, the binding energy of MP for a Mn-dilute ( $J_M \rightarrow 0$ ) NC is estimated by  $E_b \sim N_{Mn}(a_B/a)^3 \cdot 10^{-1} \text{meV}$ . This accounts for the significant increase of  $E_b$  caused by quantum confinement as  $a \sim a_B (\sim 3.1 \text{nm})$  shown in Fig. 2. On the other hand, Eq. (3) indicates that the stability of MP characterized by  $E_b$  decrease as average Mn-Mn instance decreases or Mn concentration increases. This implies that averaged magnetization of Mn-rich NCs should decrease with increasing Mn concentration, as reported by previous experiments in Refs. [5, 6]. In the analysis above, the Mn magnetization of a Mn-doped NC might be overestimated if the Mn distribution in the NC is very disordered. This is because the Mn-Mn interactions in the short range regime are much more sensitive

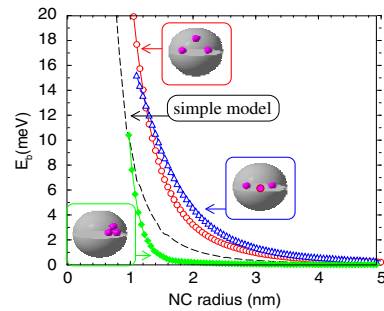


**Figure 2** Binding energies  $E_b$  of magnetic polarons (MPs) formed by three Mn ions bound by a single electron in NCs for various NC sizes and Mn position configurations. The dashed line indicates the binding energies of 3-Mn MPs in the FM phase estimated by the simplified model described by Eq. (4).

to the Mn-Mn distance than those in the long-range regime. Nevertheless, it provides us a qualitative description of the magnetic properties of uniformly Mn-doped NCs and allows us for capturing the basic underlying physics.

**3.3 Local mean field theory** For NCs with more Mn's, we employ the local mean field theory to calculate the averaged Mn magnetization for comparison of the analysis shown above [4, 13]. In the theory, the model Hamiltonian of a singly charged NC with many Mn's is written as

$$H_\sigma^{MF} = H_e - s_z h_{sd}(\mathbf{r}), \quad (5)$$

where  $H_e = |\mathbf{p}|^2/(2m^*) + V_0(\mathbf{r})$  is the non-interacting single electron Hamiltonian and  $h_{sd}$  is the local field experienced by the spin electron given by  $h_{sd}(\mathbf{r}) = J_{eM}^{(0)} n_{Mn} \langle M_z(\mathbf{r}) \rangle$  where  $n_{Mn}$  denotes the density of Mn ions. The averaged local magnetization of Mn's reads

$$\langle M_z(\mathbf{r}) \rangle = M B_M(M b(\mathbf{r})/kT), \quad (6)$$

where  $B_M$  is the Brillouin function and  $b(\mathbf{r})$  is the effective field felt by a Mn, provided by the *local* spins of other Mn ions and electron. The local spin of electron is supposed to be determined by solving the eigen problem of the single electron Hamiltonian Eq. (5), for which an iterative self-consistent calculation is needed. However, for strongly quantized NCs at sufficiently low temperature, the effective field can be simply written as

$$b(\mathbf{r}) \approx \frac{J_{eM}^{(0)}}{2} |\psi(\mathbf{r})|^2 - J_M \langle M_z(\mathbf{r}) \rangle. \quad (7)$$

Here we consider only the AF Mn-Mn interactions between the nearest neighbor (NN) Mn's and take the form of the effective AF coupling  $J_M = 6 \exp\{-\lambda[(4x_{Mn})^{-1/3} - 1]\}$ . Eq. (7) is derived under the condition where electron spin is nearly fully polarized and the influence of  $h_{sd}$  on the electronic structure of NC is neglected because of strong quantization of NC. One can show that the condition is fulfilled as  $kT \ll \langle h_{sd} \rangle \sim N_{Mn} J_{eM}^{(0)} \Omega_{QD}^{-1}$ . For the NCs considered in this work with typical volume  $\Omega_{QD} \sim 10^2 \text{ nm}^3$ , the condition is satisfied as long as  $N_{Mn} > 10$  and the thermal energy of temperature  $kT \ll 1 \text{ meV}$ .

The magnetism of a Mn-doped NC is characterized with the averaged Mn magnetization defined by

$$\langle M \rangle_{MF} \equiv \frac{1}{\Omega_{NC}} \int \langle M_z(\mathbf{r}) \rangle d^3r. \quad (8)$$

Figure 3 shows the average Mn magnetization  $\langle M \rangle_{MF}$  of Mn-doped NCs versus NC size and Mn concentration calculated by numerically solving the coupled Eqs. (5)-(7). For NCs with fixed size, average Mn magnetization  $\langle M \rangle_{MF}$  decreases monotonically with increasing Mn concentration, consistent with the analysis given by Eq. (3). Ferromagnetic MPs are stably formed in NCs (i.e.  $\langle M \rangle_{MF} \rightarrow 5/2$ ) only if the Mn concentration and NC size are sufficiently small ( $x_{Mn} < 2\%$ ) and  $a < 3 \text{ nm}$ . Under the mean field treatment, the spatially discrete magnetic moments provided by magnetic Mn ions are replaced by an effective continuous field of Mn magnetization. Thus, the MFT might overestimate the effective strength of AF Mn-Mn interactions for NCs with low Mn concentration, but underestimate that of Mn-Mn interactions for non-uniformly Mn-doped NCs with short ranged Mn-clusters. Nevertheless, the magnetic phases of magnetic NCs predicted by MFT here show similar basic features to those given by previous ED studies and analysis.

**4 Summary** In summary, we present theoretical studies of magnetic properties of magnetic polarons bound in singly charged II-VI semiconductor nanocrystals with magnetic ions  $\text{Mn}^{2+}$ . The exact diagonalization studies show that ferromagnetic magnetic polarons (MPs) are stably formed in small magnetic NCs with few long ranged Mn ions due to strong quantum confinement. By contrast,

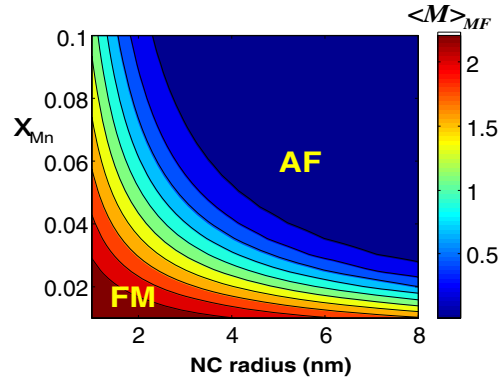


**Figure 3** Averaged Mn magnetization of magnetic NCs, calculated by the local mean field theory for  $T \rightarrow 0$ , as a function of Mn concentration  $x_{Mn}$  and NC radius.

NCs containing short ranged Mn-cluster might exhibit rich distinctive magnetic phases, from anti-ferromagnetism to ferromagnetism, sensitively depending on NC size. The stability of formation of magnetic polarons in NCs with arbitrary number of magnetic ions is analyzed within a simplified solvable model, supported by the numerical results calculated by local mean field theory.

**Acknowledgements** This work was supported by National Science Council of Taiwan under Contract No. NSC-95-2112-M-009-033-MY3.

## References

- [1] J. K. Furdyna, J. Appl. Phys. **64**, R29 (1988), and references therein.
- [2] T. Dietl, Semicond. Sci. Technol. **17**, 377 (2002).
- [3] R. N. Bhatt, M. Berciu, M. P. Kennett, and X. Wan, J. Supercond.: INM **15**, 71 (2002).
- [4] J. Fernandez-Rossier and L. Brey, Phys. Rev. Lett. **93**, 117201 (2004).
- [5] I. Sarkar, M. K. Sanyal, S. Kar, S. Biswas, S. Banerjee, S. Chaudhuri, S. Takeyama, H. Mino, and F. Komori, Phys. Rev. B **75**, 224409 (2007).
- [6] N. Feltin, L. Levy, D. Inget, and M. P. Pileni, J. Phys. Chem. B **103**, 4 (1999).
- [7] B. E. Larson, K. C. Hass, H. Ehrenreich, and A. E. Carlsson, Phys. Rev. B **37**, 4137 (1988).
- [8] F. Qu and P. Hawrylak, Phys. Rev. Lett. **95**, 217206 (2005);
- [9] Y. Z. Hu, M. Lindberg, and S. W. Koch, Phys. Rev. B **42**, 1713 (1990).
- [10] A. K. Bhattacharjee and C. Benoit a la Guillaume, Phys. Rev. B **55**, 10613 (1997).
- [11] S. J. Cheng, Phys. Rev. B **72**, 235332 (2005).
- [12] C. Gould, A. Slobodskyy, D. Supp, T. Slobodskyy, P. Grabs, P. Hawrylak, F. Qu, G. Schmidt, and L. W. Molenkamp, Phys. Rev. Lett. **97**, 017202 (2006).
- [13] R. M. Abolfath, P. Hawrylak, and I. Zutíć, Phys. Rev. Lett. **98**, 207203 (2007).